RESEARCH

Open Access

Check for updates

Cas12f1 gene drives propagate efficiently in herpesviruses and induce minimal resistance

Zhuangjie Lin[1†], Qiaorui Yao[1†], Keyuan Lai[1†], Kehua Jiao[2†], Xianying Zeng[1], Guanxiong Lei[3,4], Tongwen Zhang[1,5*] and Hongsheng Dai[1*] ◉

†Zhuangjie Lin, Qiaorui Yao, Keyuan Lai and Kehua Jiao contributed equally to this work.

*Correspondence:
vaccine-sz@outlook.com;
daihsh@outlook.com

[1] Department of Immunology, School of Basic Medicine, Southern Medical University, Guangzhou, Guangdong Province, China
[2] Department of Geriatric Medicine, Shanghai Health and Medical Center, Wuxi, Jiangsu Province, China
[3] Affiliated Hospital of Xiangnan University, Chenzhou, Hunan Province, China
[4] Key Laboratory of Medical Imaging and Artificial Intelligence of Hunan Province, Chenzhou, Hunan Province, China
[5] Vaccine Biotech (Shenzhen) LTD, Shenzhen, China, & Boji Biopharmaceutical, Guangzhou, China

Abstract

Background: Synthetic CRISPR-Cas9 gene drive has been developed to control harmful species. However, resistance to Cas9 gene drive can be acquired easily when DNA repair mechanisms patch up the genetic insults introduced by Cas9 and incorporate mutations to the sgRNA target. Although many strategies to reduce the occurrence of resistance have been developed so far, they are difficult to implement and not always effective.

Results: Here, Cas12f1, a recently developed CRISPR-Cas system with minimal potential for causing mutations within target sequences, has been explored as a potential platform for yielding low-resistance in gene drives. We construct Cas9 and Cas12f1 gene drives in a fast-replicating DNA virus, HSV1. Cas9 and Cas12f1 gene drives are able to spread among the HSV1 population with specificity towards their target sites, and their transmission among HSV1 viruses is not significantly affected by the reduced fitness incurred by the viral carriers. Cas12f1 gene drives spread similarly as Cas9 gene drives at high introduction frequency but transmit more slowly than Cas9 gene drives at low introduction frequency. However, Cas12f1 gene drives outperform Cas9 gene drives because they reach higher penetration and induce lower resistance than Cas9 gene drives in all cases.

Conclusions: Due to lower resistance and higher penetration, Cas12f1 gene drives could potentially supplant Cas9 gene drives for population control.

Keywords: Gene drive, Cas12f1, Cas9, HSV1

Background

Gene drive is a super-Mendelian inheritance in which particular genetic sequences are preferentially passed to the next generation, resulting in the dominant spread of corresponding traits within a target population [1]. Natural gene drives are mainly "selfish genes," such as transposons, homing endonuclease genes, and meiotic drive genes, and they have been modified to reduce the survival or reproduction of pests

Lin *et al. Genome Biology* (2024) 25:311

Page 2 of 20

[2]. However, these agents were not broadly adopted due to their low efficiency, poor operationality, and, most importantly, the inevitable emergence of resistance [3].

The CRISPR–Cas system has galvanized a new wave of interest in developing CRISPR-based synthetic gene drives as a tool for population control [2]. CRISPR–Cas gene-editing technique involves a Cas nuclease and a short guide RNA (sgRNA) [4–6]. Cas9 is the most widely used Cas nuclease and serves as a model for other Cas nucleases. The sgRNA has two components: a 20-nucleotide region that matches the target DNA and a scaffold that interacts with Cas9. The sgRNA guides Cas9 to a specific location in the genome by forming base pairs with the target DNA. Cas9 is then allosterically activated by the protospacer adjacent motif (PAM), a 2–6-bp sequence immediately following the target DNA sequence, and cut inside the DNA target 3–4-bp upstream of the PAM, creating a double-strand break (DSB) [7, 8].

The CRISPR-Cas9 gene drives in general are composed of (1) Cas9 nuclease and sgRNA coding sequences and (2) adjacent DNA segments (~1 kb in length on each side) that match the locus targeted by sgRNA [9, 10]. The CRISPR–Cas9 gene drive specifically induces DSB within the targeted allele and subsequently guides homology-directed repair (HDR) by using itself as the template, resulting in the integration and spread of the gene drive over generations. Gene drives based on CRISPR–Cas9 have been established in yeast [11, 12], Drosophila [9, 10], mosquitoes [13, 14], mice [15], and a human DNA virus [16].

The DSBs induced by Cas9 may also be repaired via nonhomologous end joining (NHEJ), which directly reconnects broken ends and often introduces small insertions or deletions (indels) within the sgRNA target. Because such mutated alleles lose their complementarity with sgRNA, they are no longer susceptible to the Cas9 gene drives and are called resistant alleles (Fig. 1A) [17, 18]. Resistant alleles could accumulate and eventually stop the spread of gene drives. Because of this obstacle, the use of gene drives has been limited in the laboratory mostly [17, 19, 20].

Several methods, mainly involving targeting multiple regions that are conserved or essential for a species, have been tested to reduce the occurrence of resistance to Cas9 gene drive [19, 21–23]. However, implementing these approaches is cumbersome and not necessarily effective. Another option is to explore Cas nucleases that would mechanistically induce fewer mutations at the target site after DSB repair. Cas12a is the only other Cas nuclease implemented for gene drive thus far and has been shown to propagate efficiently in yeast and fruit flies [24, 25]. However, Cas12a cuts DNA within the sgRNA target sequence [26] and is very sensitive to mismatches between the sgRNA and the target DNA [27]. In line with these properties of Cas12a, Víctor López Del Amo et al. reported that the Cas12a gene drive produced resistant alleles in 5–8% of the target population [25].

Cas12f1 is a type-V CRISPR nuclease from archaea; although it is 1/3 the size of Cas9, it has recently been engineered to achieve efficient and specific genome editing [28–30]. Cas12f1 uses a 19-nt sequence in its sgRNA to match the target DNA and then cuts at 22-nt and 24-nt upstream of the PAM [31]. Since the cleavage site for Cas12f1 is outside the base paring region of the target allele, the sgRNA target sequence could be kept intact even after the DSB were repaired by NHEJ (Fig. 1B).
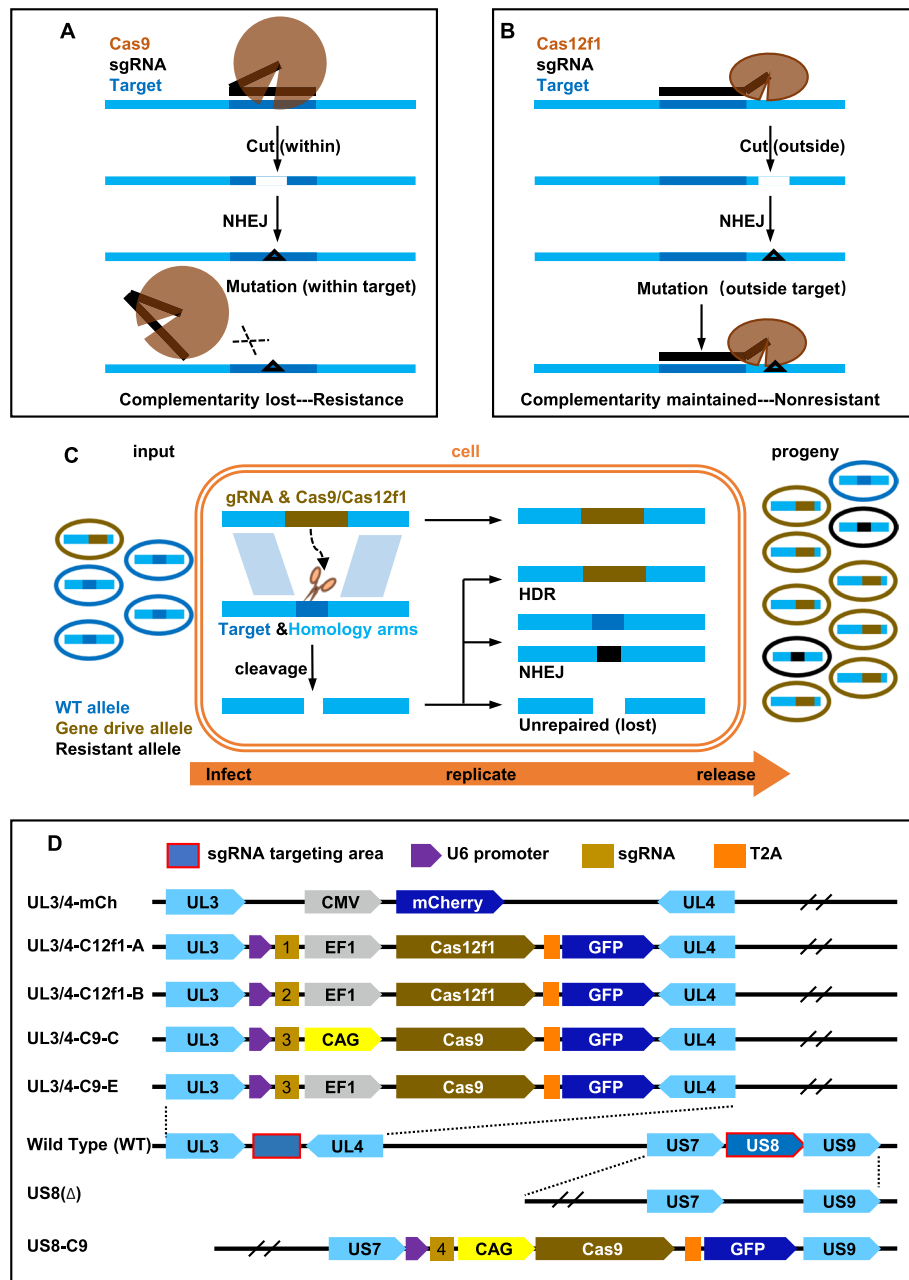
Lin *et al. Genome Biology*   (2024) 25:311

Page 3 of 20

Fig. 1 Differences between Cas9 and Cas12f1, the working model for Cas9 and Cas12f1 gene drives in HSV1, and the design of gene drive viruses. **A** The main source and consequence of mutation after genome editing by CRISPR-Cas9. **B** The main source and consequence of mutation after genome editing by CRISPR-Cas12f1. **C** The working model for viral gene drive. CRISPR-based gene drive is composed of sgRNA and Cas nucleases, such as Cas9 and Cas12f1. When HSV1 viruses with the wt allele and viruses with the gene drive allele co-infect one cell, sgRNA and Cas nuclease produced by gene drive cut the wt allele specifically at the sgRNA target locus and cause DSBs. DSBs could be repaired by HDR using the gene drive allele as the template, converting the wt allele to the gene drive. If DSBs were repaired by NHEJ, mutations might be introduced to eliminate the sgRNA targets, yielding resistant variants to the gene drive. Those unrepaired, broken genomes could not produce infectious viruses and would be eliminated. **D** Genetic map of gene drive plasmids and the resultant recombinant HSV1 viruses. Elements were not drawn in scale

Lin *et al. Genome Biology*   (2024) 25:311

Page 4 of 20

For this reason, Cas12f1 could perform multiple cycles of editing at the same locus until the complementarity between target and sgRNA is lost [28, 32].

Cas12f1's ability to undergo continuous cleavage near the sgRNA target would greatly increase the chance for the target allele to be repaired by HDR and converted to gene drive. However, Cas12f1 gene drives have not been reported thus far. In this study, we reported the creation of the first Cas12f1 gene drives, compared their performance side by side with the more conventional Cas9 gene drives, and tested if the Cas12f1 gene drives could convert all target alleles without causing resistance.

Results

HSV1 as the carrier for Cas12f1 and Cas9 gene drive

Insects were often the model organisms used to study resistance to gene drive [17, 18, 33–36]. The relatively slow pace of sexual reproduction in insects (i.e., one generation needs 10 days for flies housed at 25 ℃), however, necessitates a long time for genetic changes to spread and accumulate within such populations, making these experiments very time-consuming and difficult to scale up. It would be very helpful to have a gene drive carrier that is susceptible to genetic manipulation and has a very short reproduction cycle to support a much faster spread of gene drives.

Human herpes simplex virus 1 (HSV1), a member of the family Herpesviridae, has a linear double-stranded DNA (dsDNA) genome containing 74 open reading frames [37]. Like many other DNA viruses, each HSV1 virion contains only one copy of the genome and is considered monoploid. However, one host cell can be infected simultaneously by multiple HSV1 virions [38], each of which produces thousands of copies of the genome coexisting in the nucleus before being packaged into individual virions. Therefore, genetic materials, including gene drive, have the chance to be transferred horizontally between HSV1 genomes coexisting in one host cell (Fig. 1C). The HSV1 genome is susceptible to being edited by CRISPR–Cas9 [39, 40]. Cas9 gene drive has been shown to spread within human cytomegaloviruses (CMV), which is also a member of the herpesvirus family [16]. Therefore, it is very likely that HSV1 could carry Cas12f1 and Cas9 gene drives and support their transmission, and the short infection/replication cycle of HSV1 would make it much easier to evaluate performance and monitor resistance to gene drives in comparison with insects.

Generation of HSV1 gene drive viruses

The HSV1 dsDNA genome (~150 kb) contains many dispensable regions that can potentially harbor gene drive elements without greatly compromising HSV1's infectivity [37]. The HSV1 genes UL3 and UL4 play no essential role in HSV1 replication, and the UL3/4 intergenic region has been reported to be a safe harbor that tolerates the insertion of large DNA fragments [41]. To generate gene drive viruses with uncompromised fitness, we created gene drive cassettes to target the UL3/4 intergenic region (Fig. 1D). The two Cas12f1 genes drive *UL3/4-C12f1-A* and *UL3/4-C12f1-B* produce sgRNAs targeting different sites within the UL3/4 intergenic region (Additional file 1: Fig. S1). The two Cas9 genes drive *UL3/4-C9-C* and *UL3/4-C9-E* target the same site, but the expression of Cas9 is driven by the CAG and EF1 promoters, respectively (Fig. 1D, Additional file 1: Fig. S1). The HSV1 US8

gene encodes glycoprotein E (gE); although it is not essential for viral replication, its deficiency impairs the transmission of HSV1 between cells [37, 42]. To make gene drive viruses with defined attenuation, we constructed the gene drive cassette *US8-C9* to target the HSV1 US8 gene. We accordingly made two control cassettes: *UL3/4-mCh* with the UL3/4 intergenic region replaced with mCherry and *US8(Δ)* with a large deletion within US8 coding sequences (Fig. 1D).

Viruses *UL3/4-mCh* and *US8(Δ)* were generated by CRISPR-Cas9-assisted recombination (Fig. 2A), and the five gene drive viruses were generated by transfecting 293 T cells with gene drive plasmids described above and subsequently infecting with the HSV1 strain F (wildtype, WT hereafter) (Fig. 2B). Although autonomous homology recombination (in the absence of Cas9 and sgRNA) has long been used to modify the genome of herpesviruses [43], it occurred at very low frequency as reported in many other studies [39, 40] and hardly contributed to the generation of recombinant viruses in our reverse genetics system (Additional file 1: Fig. S2). Single clones of all engineered viruses were further purified by 3–4 rounds of plaque assay (Fig. 2C) and confirmed by junctional PCR and sequencing (Additional file 1: Fig. S3). The successful generation of gene drive viruses at high efficiency also suggested that the gene drive cassettes in the plasmids converted the target loci in the HSV1 genome as designed.

Basic properties of HSV1 gene drive viruses

Viruses *UL3/4-mCh* and *UL3/4-C12f1-A* infected and replicated like *WT* (Fig. 2D, E), confirming that the UL3/4 junction is suitable for editing. Gene drive viruses *UL3/4-C9-C* and *UL3/4-C9-E* produced plaques similar in size to those of the *WT*, but their titers were slightly lower than those of the *WT* (Fig. 2D, E). *UL3/4-C12f1-B* purified in this study produced smaller plaques and a tenfold lower titer. *UL3/4-C12f1-A* and *UL3/4-C12f1-B* had nearly identical gene drives; therefore, the decreased replication of *UL3/4-C12f1-B* was unlikely caused by the gene drive cassette itself. Due to the large size of the HSV1 genome, no attempt was made to identify the cause of the attenuated phenotype of *UL3/4-C12f1-B* or to purify other clones of *UL3/4-C12f1-B* with more favorable replication. Instead, this *UL3/4-C12f1-B* clone provided an opportunity to test if an attenuated virus could spread gene drive.

HSV1 viruses *US8(Δ)* and *US8-C9* had viral gene US8 deleted or replaced with Cas9 gene drive (Fig. 1D), and thus they lost the expression of gE as expected (Additional file 1: Fig. S4). Although *US8(Δ)* and *US8-C9* produced viral titers similar to those of the *WT* (Fig. 2E), loss of gE reduced their fitness, as seen in the much smaller plaques they formed (Fig. 2C, D).

The five gene drive viruses started to express GFP in the early stage of infection, and GFP increased in proportion to the level of HSV1 antigens as infection proceeded (Fig. 2F). GFP is linked downstream of Cas9 or Cas12f1 through T2A [44] and thus reports the production of Cas9 or Cas12f1 (Fig. 1D). Although Cas12f1 is approximately 1/3 of the size of Cas9, the additional length of Cas9 seemed to have little effect on the expression of GFP, as the levels and kinetics of GFP for all the gene drive viruses did not significantly differ (Fig. 2F).
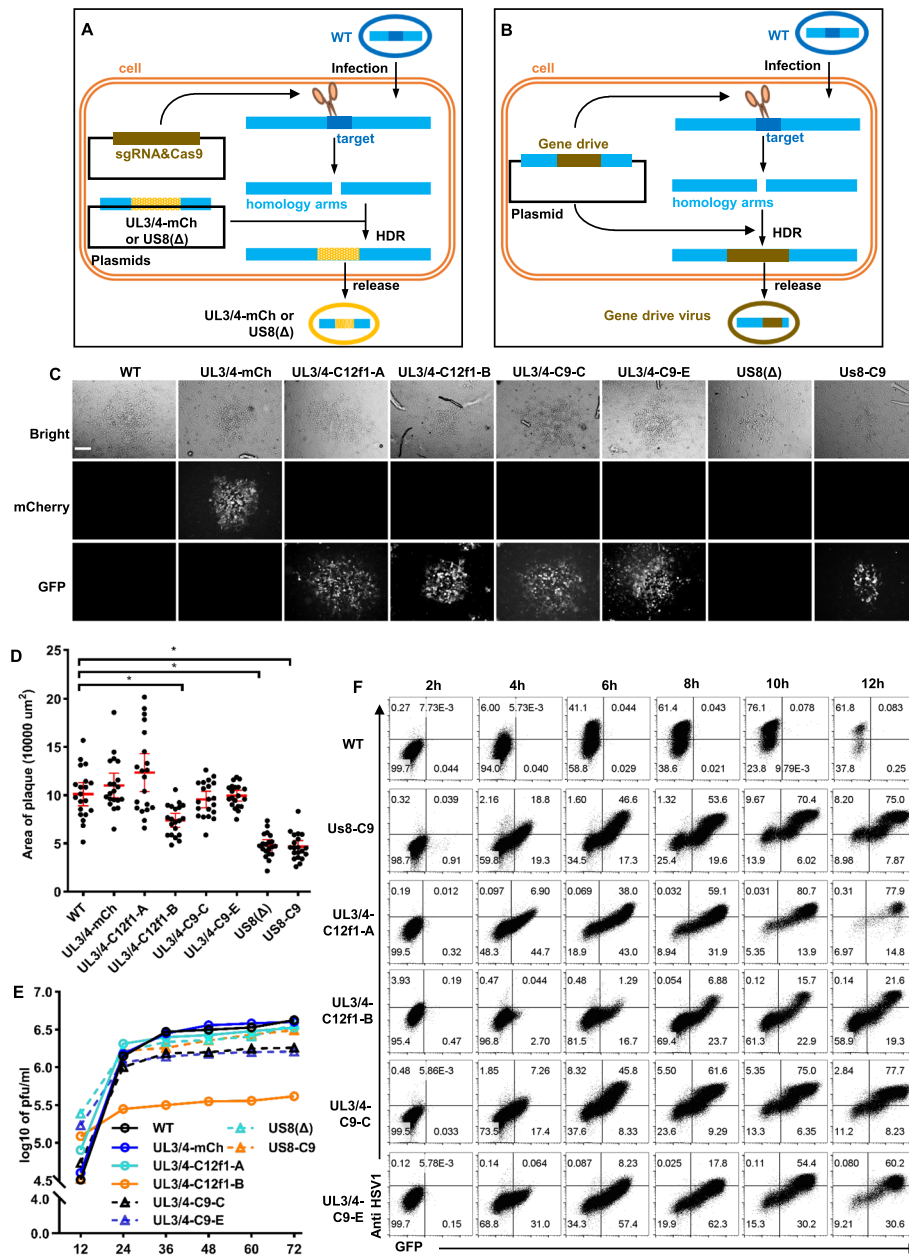
Lin *et al. Genome Biology*   (2024) 25:311

Page 6 of 20

Fig. 2 Generation and basic properties of HSV1 viruses carrying gene drives. **A** Procedures for generating recombinant HSV1 using Cas9-assisted HDR. 293 T cells were transfected with two plasmids, one plasmid encoding sgRNA and Cas9, and the other plasmid UL3/4-mCh or US8(Δ) serving as the template for HDR. **B** Procedures for generating recombinant HSV1 viruses carrying gene drive. 293 T cells were transfected with gene drive plasmids Us8-C9, UL3/4-C12f1-A, UL3/4-C12f1-B, UL3/4-C9-C, or UL3/4-C9-E, which provide Cas nuclease, sgRNA, and the template for HDR. **C** The appearance of typical plaques for each HSV1 strain on Vero cells at 48 h post infection. Scale bar, 200 μM. **D** Plaque sizes of HSV-1 viruses on Vero cells at 48 h post infection. Twenty plaques from each virus were randomly picked, and the area for each plaque was calculated and plotted. The mean with a 95% CI was marked for each virus. * indicates $P < 0.05$, which is determined by one-way ANOVA with Tukey's test. **E** One-step growth curve of HSV-1 viruses. **F** The expression of GFP and HSV1 antigens at different time points after BHK cells were infected with HSV1 viruses (MOI = 2)

Gene drive could spread among HSV1 viruses in a target-dependent manner

Although multiple HSV1 virions can infect the same host cell and create the opportunity for viruses with different genomes to exchange genetic materials, transmission of gene drives among HSV1 viruses has not been tested as the time of writing. *UL3/4-mCh* (mCherry +) and *US8-C9* (GFP +) viruses have distinct phenotypes, and *UL3/4-mCh* viruses have intact US8 coding sequences to be targeted by gene drive *US8-C9* (Figs. 1D and 2C). To test the spread of gene drive among HSV1 viruses, we first performed coinfection of US8-C9 and UL3/4-mCh in Vero cells (Fig. 3A1). The chimeric viruses that express both GFP and mCherry emerged after one cycle of coinfection and comprised more than 50% of the total viral population after three cycles of coinfection (Fig. 3B, D). Their plaques are smaller than those of *UL3/4-mCh* but close to those of *US8-C9* (Fig. 3E), a phenotype consistent with gE deficiency. Furthermore, junctional PCR showed that the chimeric virus had both *UL3/4-mCh* and *US8-C9* gene drives in the correct loci (Fig. 3F). These results clearly demonstrated that gene drive could transmit among HSV1 viruses. Although we mostly used Vero cells for convenience as the host for HSV1 coinfection, we also determined that primary mouse embryonic fibroblasts (MEFs), which were susceptible to recombinant HSV1 viruses (Additional File 1, Fig S5), supported invasion of the viral gene *US8-C9* drive into *UL3/4-mCh* (Additional File 1, Fig S6). The spread of viral gene drive is thus not restrictive to Vero cells.

On the other hand, we tested coinfection with WT virus (gD$^+$, GFP-) and each strain of gene drive viruses (gD$^+$, GFP$^+$), respectively, and determined the composition of viruses after each cycle of coinfection via fluorescence staining (Fig. 3A2). Although the four gene drive viruses *UL3/4-C12f1-A*, *UL3/4-C12f1-B*, *UL3/4-C9-C*, and *UL3/4-C9-E* replicated at a level close to or even lower than that of the *WT* viruses (Fig. 2E), their percentages in the total viral population all increased steadily from ~25% at P0 to ~70% at P2 (Fig. 3G). To test if such a biased expansion of gene drive viruses is related to the UL3/4 intergenic region, for which the four gene drives targeted, we also coinfected *UL3/4-mCh* (mCherry$^+$) with each of the four gene drive viruses (GFP$^+$) targeting the UL3/4 intergenic region (Fig. 3A3). *UL3/4-mCh* had the UL3/4 intergenic region replaced with mCherry and showed similar replication dynamics as WT (Figs. 1D, and 2E). Under this condition, the percentage of *UL3/4-mCh* and each strain of gene drive virus after each passage was within a range close to their initial proportion in the viral population, and no viruses expressing both mCherry and GFP were observed (Fig. 3H, Additional file 1: Fig. S7). Therefore, the biased expansion of the four gene drive targeting the UL3/4 intergenic region over *WT* viruses is related to their specific target.

Using *WT* HSV1 as the recipient of the four gene drives should produce progeny gene drive viruses that are genetically and phenotypically indistinguishable from the input gene drive viruses. The biased expansion of gene drive viruses *UL3/4-C12f1-A*, *UL3/4-C12f1-B*, *UL3/4-C9-C*, and *UL3/4-C9-E* could be contributed by converting the *WT* UL3/4 intergenic region into gene drive and by eliminating the *WT* viral genome—cutting genome without repair (Fig. 1C). Because it is hardly possible to quantify the lost unrepaired genome, it is inherently challenging to parse out the exact individual contribution of converting or eliminating targets by any gene drive (Fig. 3A1–A2). However, based on our successful generation of viruses carrying gene drives and clear demonstration of the transmission of gene drives *US8-C9* among HSV1 viruses, we believed that
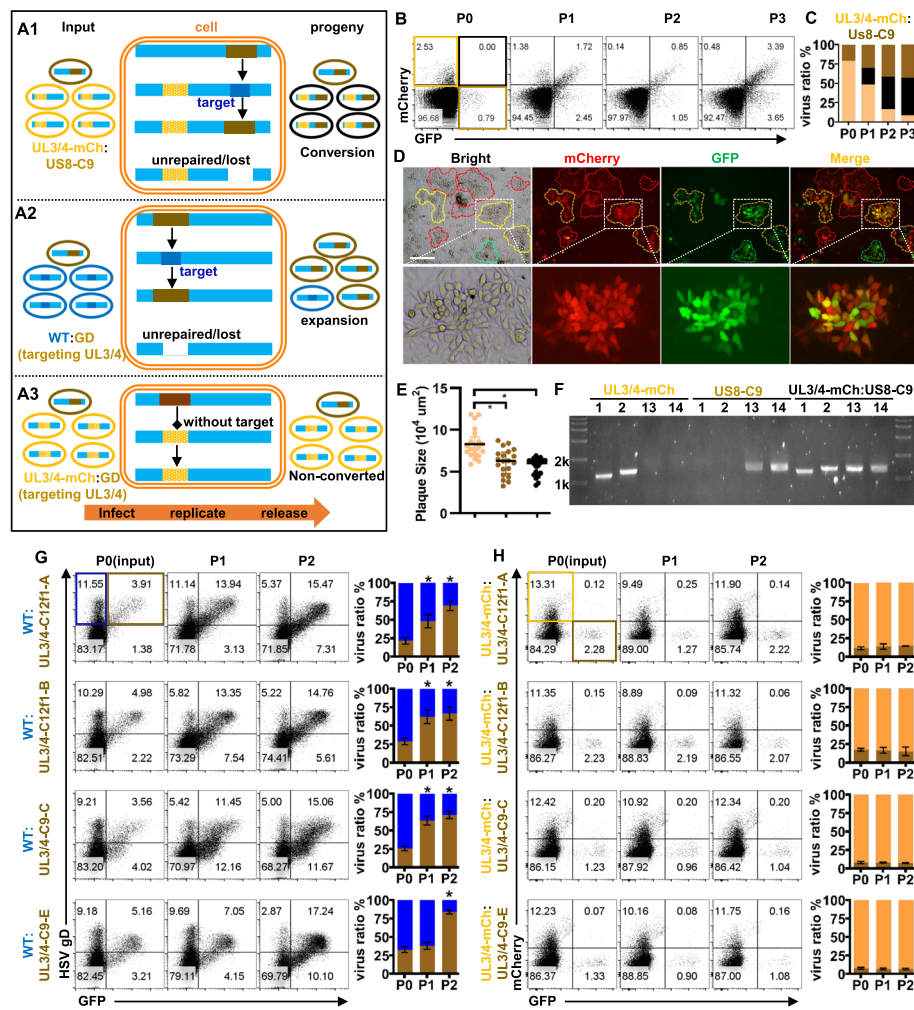
Lin *et al. Genome Biology*   (2024) 25:311

Page 8 of 20

Fig. 3 Target-specific spread of gene drive in HSV1 viruses. **A** Schematic diagrams show the possible consequences of the coinfection of HSV1 viruses. Cas nuclease would cut HSV1 genome at the target site, and the broken HSV1 genome may be repaired and converted to progeny gene drive or resistant variants, or it may not be repaired. Unrepaired broken genomes would be lost eventually. In the absence of the target, the spread of gene drive may cease. **B-C** *UL3/4-mCh* and *US8-C9* (MOI = 5, *UL3/4-mCh*: *US8-C9* ≈4:1) were applied to infect Vero cells, and supernatants were collected 24 h post-infection and used to infect fresh Vero cells. This procedure was repeated as necessary to help the spread of gene drives. The ratio of each strain of viruses at P0 (input), P1 (first round infection), P2 (second round), and P3 (third round) was determined by infection of BHK cells at MOI≈0.1 for 12 h and then analyzed by flow cytometry. *UL3/4-mCh* was shown or gated as red, *US8-C9* as green, and chimeric viruses as yellow. Representative flow cytometry graphs (**B**) and the average ratios of each strain (**C**) of two independent experiments are shown. **D**, **E** Representative image and sizes of plaques from P1 supernatant of *UL3/4-mCh:US8-C9* coinfection. Plaques were imaged for the expression of fluorescent proteins (**D**), grouped based on their fluorescent pattern and measured for their size (**E**) (*n* = 20, *P < 0.05, calculated by one-way ANOVA with Tukey's test). Scale bar, 500 μM. **F**. PCR fragments showing the transmission of gene drive to the target site. PCR fragments were amplified from single clones purified from **D**. with specified primer sets (see Additional file 1, Fig S3 for primer sets). **G** *WT* (GFP-, gD +) and gene drive viruses (GFP +, gD +) coinfection was performed and measured as in **B**. *WT* was shown or gated as blue, *gene drive* as green. **H** *UL3/4-mCh* (mCherry +) and gene drive virus (GFP +) coinfection was performed as in **B** but with an introduction frequency of 5%. *UL3/4-mCh* was shown or gated as red and gene drive as green. Representative flow cytometry graphs and statistical summaries of three experiments are shown for **G** and **H**, * indicates *P < 0.05 by comparing with Passage 0 (one-way ANOVA with Tukey's test)

Lin *et al. Genome Biology*   (2024) 25:311

Page 9 of 20

the four gene drives targeting the UL3/4 intergenic region converted their targets with good efficiency, which would be further corroborated with different experimental settings in the remaining study.

Transmission dynamics of the Cas12f1 and Cas9 gene drives

We next sought to compare Cas12f1 and Cas9 gene drives and sort out their functional differences by using *US8(Δ)* as the recipient for the four gene drive viruses targeting UL3/4. The progeny gene drive viruses were gD + ,GFP + ,gE- and readily distinguishable from the input gene drive viruses, which were gD + ,GFP + ,gE + (Fig. 4A). It should be noticed that fluorescent staining could not differentiate the input *US8(Δ)* and its variants with resistance to gene drive.

We coinfected *US8(Δ)* with each gene drive virus at initial ratios of 4:1 and 19:1 to simulate different levels of transmission threshold, and tracked the conversion of *US8(Δ)* to gene drive after each passage. In all cases, the Cas12f1 gene drives and the Cas9 gene drives steadily invaded *US8(Δ)* viruses and produced progeny gene drives (yellow columns) that became the most abundant species after a few passages (Fig. 4B–I). The two Cas12f1 gene drives were able to convert almost all *US8(Δ)* viruses by P7 at the initial ratio of 4:1 (Fig. 4B–C); however, 4 more cycles of confection were needed for the near-complete conversion of *US8(Δ)* by the Cas12f1 gene drives at the introduction frequency of 5% (Fig. 4F, G).

Cas9 gene drives failed to invade a significant portion of *US8(Δ)*, which may have acquired mutations to resist gene drive and even gradually rebounded starting from P5 (Fig. 4D, E and H, I). The spread of Cas9 gene drives were not slowed down much at the introduction frequency of 5%; they still reached equilibrium with *US8(Δ)* after 5 passages (Fig. 4D, E and H, I). Plotting together the percentages of *US8(Δ)*-derived gene drive viruses after each passage showed that Cas12f1 gene drives and Cas9 gene drives had similar conversion efficacy at the introduction frequency of 20% (Fig. 4J), and Cas12f1 gene drives behaved less invasively than Cas9 gene drive at the introduction frequency of 5% (Fig. 4K). Because these four gene drives have the same homologous arms, any discrepancy shown in their transmission should originate from Cas9 and Cas12f1. The lower invasiveness of Cas12f1 gene drive at low introduction frequency may be explained because Cas12f1 had lower editing efficacy than Cas9 [28–30].

The input gene drive viruses were all gradually superseded by *US8(Δ)*-derived gene drive viruses after several passages (Fig. 4B–I). This is likely because *UL3/4-C12f1-B*, *UL3/4-C9-C*, and *UL3/4-C9-E* all produced lower virus titers than *US8(Δ)* (Fig. 2E) and thus were eventually outcompeted by *US8(Δ)*-derived gene drive viruses. However, how UL3/4-C12f1-B was displaced by *US8(Δ)*-derived gene drive viruses during coinfection is yet to be determined.

Genetic changes caused by Cas9 and Cas12f1 gene drive

To examine how the spread of gene drive could change the genome of remaining *US8(Δ)* viruses and result in resistance, we sampled the 4:1 coinfection at P0 (input), P1, P4, and P7, amplified the UL3/4 intergenic region, and performed deep sequencing (Fig. 4A). The two primers used to amplify the UL3/4 intergenic region bind at the 3′ end of the coding sequences of UL3 and UL4, respectively, and thus could pair with both genomes
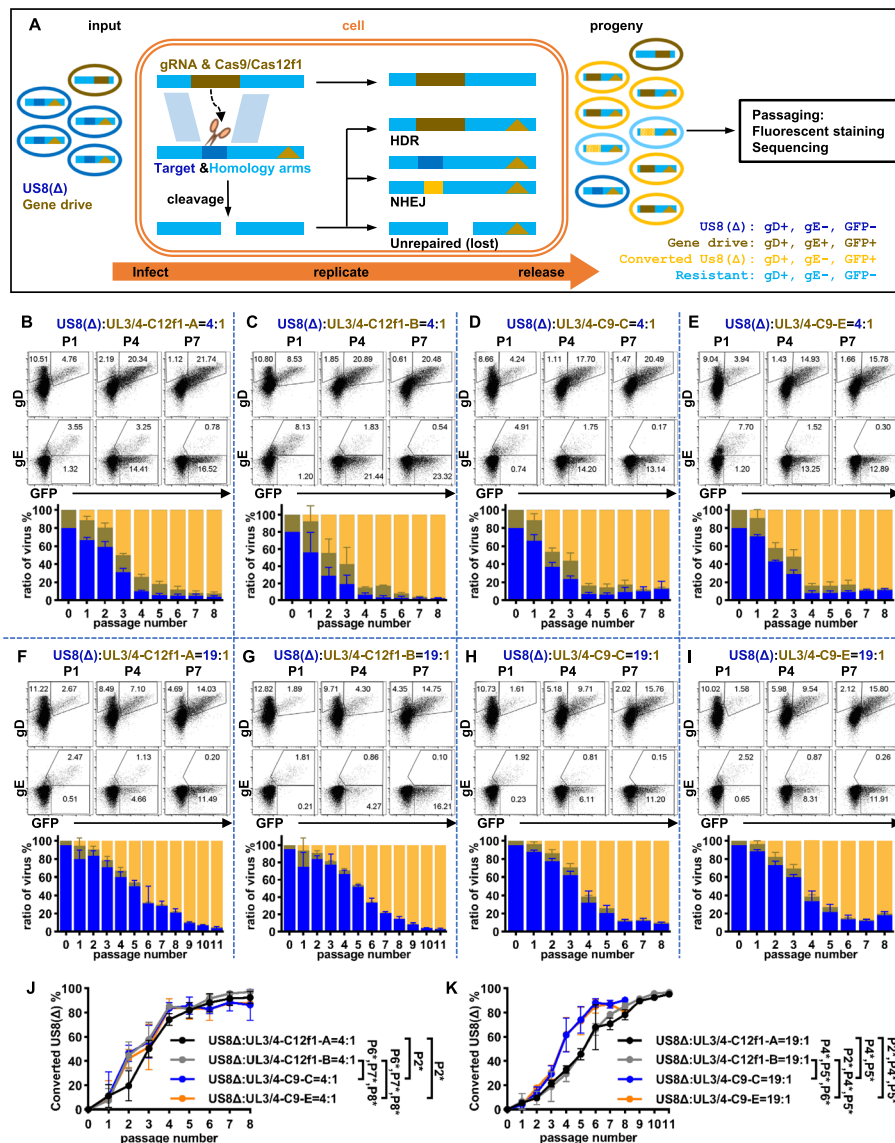
Lin *et al. Genome Biology* (2024) 25:311

Page 10 of 20

Fig. 4 The transmission dynamics of the Cas12f1 and Cas9 gene drives in HSV1 viruses. **A** A schematic diagram shows the procedure and possible consequences of coinfection of gene drives and *US8(Δ)* viruses. During coinfection, *US8(Δ)* could be converted to a new generation of gene drive viruses, become resistant variants, or be lost if a broken *US8(Δ)* was not repaired. Coinfection could be passed over fresh host cells for multiple rounds as necessary. The ratio of progeny gene drive after each passage could be determined by fluorescent staining according to their distinct patterns, and the emergence of resistant clones could be assessed by deep sequencing. **B–K** Invasion of gene drive into *US8(Δ)* was conducted with an introduction frequency of 20% (*US8(Δ)*: gene drive = 4:1) (**B–E** and **J**) or 5% (*US8(Δ)*: gene drive = 19:1) (**F–I** and **K**). Shown are representative staining (upper panel) and the percentages of each strain of virus (lower panel) after each passage. The blue, green, and yellow bars represent *US8(Δ)* viruses, the input gene drive viruses, and progeny gene drive viruses derived from *US8(Δ)* viruses, respectively. The percentages of progeny gene drive viruses at each passage from each coinfection were plotted as mean ± SD for the introduction frequency of 20% (**J**) or 5% (**K**). *P*-values were determined by one-way ANOVA with Tukey's test (*n* = 4), and comparison between passages with *P* < 0.05 were marked with * (**J**, **K**)

of *US8(Δ)* and gene drive viruses. A short extension time (20 s) was used to restrict the PCR to amplify only the UL3/4 intergenic region of *US8(Δ)*. Under this condition, the coexisting genomes of gene drive viruses could still absorb the primers, interfere with
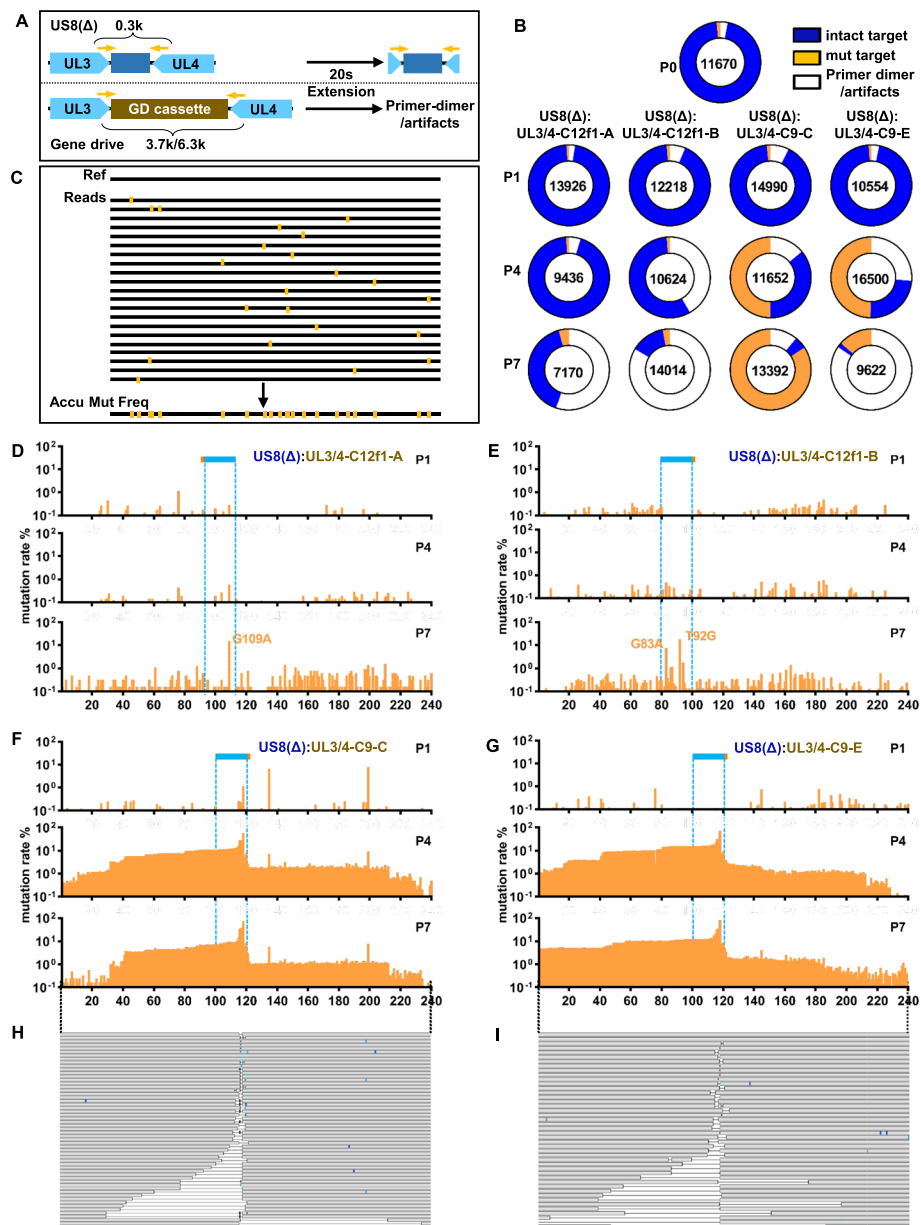
Fig. 5 Cas12f1 and Cas9 gene drives produced distinct patterns of mutation and resistance. **A** PCR procedure for restrictively amplifying the UL3/4 intergenic region for deep sequencing. **B** The UL3/4 intergenic region was amplified from input viruses (P0) or supernatants collected after coinfection and applied for deep sequencing. The colored cycle showed the relative ratios of three types of reads, and inside each cycle were the total number of reads for each sample. **C**–**G** Mutations from each read that could be mapped to the UL3/4 intergenic region were piled up to show their distribution and relative frequency along the reference sequences. Schematic diagram of analysis (**C**) and distribution and frequency of mutations accumulated at the UL3/4 intergenic region for coinfection *US8(Δ):UL3/4-C12f1-A* (**D**), *US8(Δ):UL3/4-C12f1-B* (**E**), *US8(Δ):UL3/4-C9-C* (**F**), and *US8(Δ):UL3/4-C9-E* (**G**). The locations of the sgRNA target sequences and the PAM are marked with blue-red bars. **H**, **I** Nonredundant indels from P7 of US8(Δ):UL3/4-C9-C (**H**) or US8(Δ):UL3/4-C9-E (**I**) were mapped to the reference sequences. Each bar represents a unique read, breaks linked by dashed lines are deletions, and sporadic blue marks represent point mutations

PCR amplification, and yield aborted PCR fragments (i.e., primer-dimers), especially when their presence is significant and *US8(Δ)* is low (Fig. 5A). We indeed observed a large number of short aborted PCR fragments that could not be mapped to the reference UL3/4 intergenic sequences in some P4 and P7 samples (Fig. 5B). This is consistent with fluorescent staining results that showed these samples generally had a dominant presence of gene drive viruses and low *US8(Δ)* (Fig. 4B–E).

We next examined for mutations in all sequencing reads that correctly aligned to the UL3/4 intergenic region and first focused on the short sequences that each gene drive targeted (Additional file 1: Fig. S1). The input *US8(Δ)* viruses (P0) were originally purified from a single plaque; however, we found that up to 1.5% of all reads of the input *US8(Δ)* (P0) contain mismatches within any one of the three sgRNA target sequences (Fig. 5B). These mismatches involved mostly single nucleotides and were scattered randomly; some of these mismatches may be true mutations that emerged as a result of fast replication of HSV1 [45], and some of these mismatches may be inherent errors of PCR and sequencing [46]. Both Cas9 and Cas12f1 have good tolerance to single point mutations within their sgRNA target [6, 28]. The very small portion of *US8(Δ)* viruses with no decisive mutations is unlikely to hamper the whole *US8(Δ)* population as the recipient of gene drive, although the possibility exists that some very rare variants with critical point mutations could be positively selected during coinfection with gene drive viruses.

The percentage of reads with any mutation within sgRNA targets did not increase significantly after the first cycle of coinfection with any of the four gene drive viruses (P1 vs. P0) (Fig. 5B). As more cycles of coinfection occurred, however, Cas12f1 gene drives and Cas9 gene drives exhibited great differences in altering the sgRNA targets and neighboring sequences of *US8(Δ)*. The two Cas12f1 gene drives converted almost all *US8(Δ)* viruses and left only a tiny fraction of the input *US8(Δ)* after 4 or 7 passages (Fig. 4B, C). Although the percentages of reads with mutations within the two Cas12f1 sgRNA targets increased after 7 cycles of coinfection (P7 vs. P0), the majority of the remaining *US8(Δ)* viruses still had intact sgRNA targets and thus were susceptible for the next round of editing. As for the two Cas9 gene drives, the remaining *US8(Δ)* had lost most sgRNA targets by P4 and nearly all of them by P7 (Fig. 5B).

We also analyzed the cumulative mutation rate for each base across the whole UL3/4 intergenic sequences (Fig. 5C). The vast majority of mutations present on the remaining *US8(Δ)* viruses after coinfection with the two Cas12f1 gene drives were point mutations, which were scattered without apparent hotspots for the P1 and P4 samples. As more infection and replication cycles happened, however, more mutations accumulated, and three dominant clones with point mutations within sgRNA target sequences emerged in P7 samples (Fig. 5D, E). The G109A mutation was located in the sgRNA target of *UL3/4-C12f1-A* gene drive, and its frequency increased from 0.3% in P1 to 8.3% in P7 (Fig. 5D). The G83A and T92G mutations caused mismatches in the gene drive *UL3/4-C12f1-B* (Fig. 5E). These three point mutations are not close to the breakpoints where the Cas12f1 cuts and NHEJ repairs. It is unlikely to attribute these mutations to Cas12f1 gene drive; they may occur naturally in the first place and be positively selected later for their resistance to Cas12f1 gene drive.

No distinct change to the UL3/4 intergenic sequences of *US8(Δ)* viruses was observed after one cycle of coinfection with the two Cas9 gene drives (Fig. 5F, G). However, the

remaining *US8(Δ)* viruses in the P4 and P7 samples had many short indels in their UL3/4 intergenic sequences, and these indels were centered on the third nucleotide upstream of the PAM (Fig. 5F, G), the place where Cas9 nuclease usually cuts DNA [7]. Error-prone repair of DSB by NHEJ often produces short indels near the breakpoint and is the main source of mutations during the transmission of gene drives. Therefore, these genetic insults to the remaining *US8(Δ)* viruses are the result of failed transmission of the Cas9 gene drives. We also found that large deletions (loss > 50 nt) appeared in 3–7% of the reads. However, they were not equally distributed around the cut site of Cas9. The 5′ side of the breakpoint was truncated more frequently than the 3′ side, and there were almost no reads with large deletions across both sides of the breakpoint (Fig. 5H, I).

Deep sequencing results were consistent with the changes of *US8(Δ)* viruses shown with fluorescent staining and clearly explained why conversion of *US8(Δ)* by the two Cas9 gene drives were ceased after P5 and why conversion of *US8(Δ)* by the two Cas12f1 gene drives preceded without restraint.

Discussion

Walter and Verdin et al. recently reported their development and characterization of Cas9-based HSV1 gene drive viruses targeting a different locus of the HSV1 genome and shown that Cas9 gene drives left up to 20% of the remaining target sites mutated by NHEJ [47]. This is in line with our findings regarding Cas9 gene drive and highlights the importance of developing gene drive mechanisms to avoid the occurrence of resistance.

In this study, we generated HSV1 viruses that carried functional Cas9 and Cas12f1 gene drives. Due to the rapid replication of HSV1, the spread of gene drive proceeded at a speed not achieved in any other organisms tested thus far [12, 15, 16, 25]. Both Cas9 and Cas12f1 gene drives were highly effective and capable of converting targets even when their introduction frequency was low. The Cas9 gene drives produced a high percentage of resistant viruses by introducing mutations at the target sites; the Cas12f1 gene drives instead were able to convert almost all targets without causing many resistant clones, although it is possible that resistance for the Cas12f1 gene drive would accumulate after more rounds of coinfection.

Cas12f1 cuts the target DNA at 22-nt and 24-nt upstream of the PAM [31], which intrinsically preserves the sgRNA target sites and allows multiple editing at the same locus [28, 32]. Previous studies showed that Cas12f1 caused fewer mutations than Cas9 while editing the genome of 293 T cells, and the resultant mutations were mainly deletions around the target [28, 32]. In the first Cas12f1 viral gene drive study, we barely observed any deletional mutations near the target sites of the Cas12f1 gene drive. It is unlikely that we failed to detect such indels, because our amplicon NGS sequencing protocol reliably detected a wide range of indels caused by Cas9 gene drives. Cas12f1 cuts dsDNA and leaves sticky ends [31], which has been reported to help with HDR when there is a matching template [48]. When HSV1 viruses replicate inside host cells, thousands of copies of the genome are produced. This means that there are many templates available for HDR, both from the wild-type and the gene drive versions of HSV1. The sticky ends generated by Cas12f1 and the availability of ample repair templates may contribute to nearly 100% of the conversion rate of the Cas12f1 gene drives in HSV1.

Lin *et al. Genome Biology*   (2024) 25:311

Page 14 of 20

It would be worthwhile to investigate whether Cas12f1 gene drive could achieve such a high conversion rate in other organisms.

We noticed that Cas9 gene drive *UL3/4-C9-C* and *UL3/4-C9-E* had produced some resistant *US8(Δ)* clones that had large deletions in their genomes. These large deletions occurred dominantly at the 5′ side of the break point of the target sequences. Unidirectional editing is a property of type I-E CRISPR nucleases Cas3, which induces large deletions mostly upstream of the PAM [49]. However, this property has not been previously reported for Cas9. Since *UL3/4-C9-C* and *UL3/4-C9-E* targeted the same sequences, we could not rule out that such a deletion pattern is specific to this target site. Testing Cas9 gene drives targeting other regions of the HSV1 genome may help determine if Cas9 preferentially introduces large deletions to the 5′ side of the DSB.

In insects and higher organisms, the spread of gene drive occurs as the result of sexual reproduction. For this reason, gene drives with high fitness costs often decrease the fecundity of the carrier organism and fail to spread in a population, and great efforts have been invested in reducing the fitness cost of gene drives [13, 50]. Transmission of viral gene drives in this study occurs among HSV1 viruses that replicate asexually inside one host cell. It is common that HSV1 viruses with non-overlapping defects compensate for each other when coinfecting one cell [38, 51]. If for any reason the viruses that carried gene drive showed reduced fitness, no matter if it was caused by gene drive itself or not, compensation by coexisting normal alleles in the same cell could mitigate the negative impact of reduced fitness. In other words, the functional compensation among viruses could greatly buffer the impact of the fitness costs of a gene drive on its transmission among HSV1 viruses. This may explain why gene drive virus *UL3/4-C12f1-B*, which had much reduced fitness as shown in its smaller size of plaque and lower titer (Fig. 2C–E), converted its targets (*WT* and *US8-C9*) as efficiently as the wild-type like virus *UL3/4-C12f1-A* (Figs. 3A, and 4B, C). Although it is also possible that the reduced fitness of *UL3/4-C12f1-B* here is not severe enough to significantly affect the spread of gene drives.

Cas9-based gene drive has been reported for HCMV [16]. Although both HCMV and HSV1 are herpesviruses, HSV1 replicates much faster and at higher titers than HCMV [52]. We initially suspected that the short replication cycle of HSV1 might pose a challenge for the transmission of gene drive, as it might be too short to complete a multistep process involving the production of sgRNA and Cas nuclease, cleavage of the target, and DSB repair by HDR. Both the Cas9 and Cas12f1 gene drives spread very efficiently among HSV1 viruses, suggesting that such viral gene drives would also work for other herpesviruses, most of which usually replicate at a pace falling in between CMV and HSV1.

Genome editing has long been attempted to control HSV1 infection [53], and recent advances have included more effective delivery of sgRNA/Cas9 and meganucleases [54, 55]. It is tempting to postulate that HSV1 gene drive could also be a new type of intervention to treat herpes infection. However, the long-lasting risk of off-target editing to the genome of host cells and the fact that HSV1 infection in general is self-limiting would restrict the use of gene drive and other genome editing therapies in those rare cases of repetitive and refractory infection. HSV1 is a safe and versatile vector, as engineered HSV1 viruses have been approved for treating cancer [56] and genetic diseases

Lin *et al. Genome Biology*   (2024) 25:311

Page 15 of 20

[57]. HSV1 could alternatively be engineered to carry gene drives targeting other more harmful herpesviruses, such as HSV2, CMV, and EBV, and curatively treat their latent infection. Furthermore, the therapeutic potential of the resistant-proof Cas12f1 gene drive could be greatly broadened should a safe off-target profile of Cas12f1 (or a better version of Cas12f1) be established. In comparison with Cas9, very little is known for the specificity and accuracy of Cas12f1. Defining off-target editing of Cas12f1 and engineering safer Cas12f1 are worth extra efforts in the future.

Overall, our study presented the first Cas12f1-based gene drive and established HSV1 as a useful vector for studying horizontal gene transfer. Although HSV1 could not model complex traits of higher organisms, such as sex conversion, the fast replication cycle of HSV1 would be very useful for characterizing transmission dynamics and the occurrence of resistance to gene drive. Just like in other ecological systems, many different types of competition and cooperation exist among viral populations [58]; how these interweaved interactions affect the spread of gene drive could have great significance for the various applications of viral gene drive and warrant further study.

Conclusions

The first Cas12f1 gene drives were generated in HSV1 and compared with the Cas9 gene drive. Cas12f1 gene drive performed better than Cas9 gene drive because it induced low resistance. HSV1 supported faster transmission of both Cas9 and Cas12f1 gene drives and could be a general carrier to rapidly determine some basic properties of gene drives, such as transmission dynamics and the occurrence of resistance.

Methods

Cells and viruses

Authenticated HEK293T, BHK-21, and Vero cells and the HSV-1 F strain were obtained from the American Type Culture Collection (ATCC). HEK293T, BHK-21, and Vero cells were cultured in DMEM supplemented with 10% fetal bovine serum (FSP500, ExCell Bio) and 10,000 U/ml penicillin/streptomycin (BL505A, Biosharp) and maintained at 37 °C with 5% CO_2. MEF cells (iCell-m033) were purchased from iCell and cultured in D/F12 supplemented with 10% FBS. Cell lines were surveyed monthly for mycoplasma contamination (MycoBlue Mycoplasma Detector, Vazyme).

Construction of gene drive cassettes

sgRNA targets were selected using the online tool CRISPOR (http://crispor.tefor.net/), and all plasmids were designed using SnapGene® software (Dotmatics; available at snapgene.com). Cas9 was amplified from px330 (Addgene), and Cas12f1 was derived from the optimized Cas12f1 sequence [28] and synthesized (General Biol). The vector backbone and insert fragments were amplified with Q5 high-fidelity DNA polymerase (M0491L, NEB) and ligated together with the ClonExpress® Ultra One Step Cloning Kit (C112-02, Vyzame). Ligation products were subsequently transformed with DH10B competent bacteria, after which single clones were picked and validated via Sanger sequencing (Tsingke). The sequences and annotations of all the plasmids used in this study are available upon request.

Lin *et al. Genome Biology*   (2024) 25:311

Page 16 of 20

Generation of the HSV1 gene drive virus

First, 293 T cells were transfected with gene drive plasmids precomplexed with PEI (408,727-100ML; Sigma−Aldrich), cultured for 12 h, and subsequently infected with the HSV-1 F strain (MOI = 0.1). The recombination of plasmids and viruses was allowed to continue for 48 h, after which the virus-containing supernatants were harvested. To isolate recombinant viruses, a single layer of Vero cells was infected with sequentially diluted supernatant for 1 h and overlaid with 1% methylcellulose (C6333-250 g, Macklin) solubilized in DMEM. Individual plaques expressing the reporter gene were picked at 48 h and propagated and purified by an additional 3 to 4 rounds of plaque assay. The genomic DNA of individual clones was extracted with a DNA extraction kit (DC102, Vazyme), amplified with primers (Additional File 2, Table 1), and validated by Sanger sequencing (Tsingke).

Titration of viruses

Viral titration was conducted as previously described [37]. Briefly, 2×10^4 Vero cells were incubated with sequentially diluted viruses at 37 °C for 4 h. Human gamma globulin, which contains polyclonal antibodies against HSV1, was added to the culture to a final concentration of 0.5% (v/v). After 48 h, the plaques were counted under an inverted microscope.

Imaging

Pictures of viral plaques were taken at 48 h post-infection with a Nikon Eclipse Ts2-FL inverted microscope. To compare the plaque sizes of the different viruses, 20 plaques were randomly picked from each virus, and the area of each plaque was calculated using Nikon acquisition software, NIS-Elements BR 5.30.0364.

Purification of viruses

To prepare virus stocks, BHK-21 or Vero cells were infected with the HSV1 F strain or its derivatives at an MOI of 0.1. Both cells and supernatants were harvested when cytopathic effects were observed in all cells. The cells were subjected to three freeze–thaw cycles to release the viruses. Cell debris was removed by centrifuging at $6000 \times g$ for 20 min. The cleared supernatant was layered on 30% sucrose and further purified by centrifugation at $12,000 \times g$ for 2 h. The viruses were resuspended in PBS and subsequently aliquoted, titrated, and stored at -80 °C until use.

Growth kinetics of viruses

Vero cells seeded in 24-well plates were infected with viruses (MOI = 0.1) for 1 h at room temperature. After washing with PBS, the cells were further cultured in DMEM supplemented with 5% FBS. Supernatants were collected at 12, 24, 36, 48, 60, and 72 h after infection. Viral titers were determined by plaque assay.

Continuous transmission of gene drive

Vero cells or MEFs were infected with target viruses and gene drive viruses (total MOI≈5, target: gene drive≈4:1). According to the Poisson distribution, such

coinfection conditions meant that a host cell had a 63% probability of being simultaneously infected by the WT strain and at least one gene drive virion. In some cases, additional coinfection with a target: gene drive of 19:1 was also conducted. Supernatants were harvested 24 h after each cycle of coinfection. Their viral titers were estimated based on the growth curve of each strain of virus. Supernatants were used to infect fresh Vero cells or MEFs at MOI≈5 for new cycles of coinfection as needed. To quantify the ratios of each strain of virus, supernatants harvested from each passage were diluted and used to infect fresh BHK cells at MOI≈0.1 for 12 h. The infected cells were stained with monoclonal antibodies against HSV1 gD (sc-21719, Santa Cruz) or gE (sc-69803, Santa Cruz) and a matching fluorescent secondary antibody (A0473, Beyotime). Samples were collected via flow cytometry (NovoCyte, Agilent). The flow cytometry results were analyzed using FlowJo™ V10.8 (BD Life Sciences).

NGS amplicon sequencing and analysis

PCR fragments were amplified by specific primers with adaptors (Additional file 1: Fig. S1). Equimolar PCR products of 2 replicates of the same passage were pooled together and then ligated to distinct barcoded adapters and sequenced with a read length of 150 nt from both sides with the Illumina MiSeq PE150 platform (Tsingke). The paired-end sequencing raw data were first checked for quality by FastQC v0.11.9 (https://www.bioinformatics.babraham.ac.uk/projects/fastqc/) and subsequently analyzed with the commercial software Geneoious Prime 2023.2.1 (https://www.geneious.com). The reference sequences were provided in Additional file 1: Fig. S1. The data were trimmed and mapped to reference sequences. After removing primer dimers, a neighbor-joining tree was constructed for all the mapped reads using the Tamura–Nei model. The mutation rate at each nucleotide of the reference sequences was determined from the phylogenetic tree. Indels were defined as small indels (< 50 bp) or large indels ($\geq$ 50 bp).

Statistics and reproducibility

The percentage, mean, CI, and standard deviation were calculated using GraphPad Prism 9.5. The sample size was not predetermined, and no data were excluded from the analyses. The experiments were not randomized, and the investigators were not blinded to the allocation of the studies during the experiments or outcome assessment.

Supplementary Information

The online version contains supplementary material available at https://doi.org/10.1186/s13059-024-03455-9.

Additional file 1: Supplementary figure S1-S7.

Additional file 2: Supplementary table S1-S2.

Additional file 3. Review history.

Peer review information
Kevin Pang and Wenjing She were the primary editors of this article and managed its editorial process and peer review in collaboration with the rest of the editorial team.

Review history
The review history is available as Additional file 3.

Lin *et al. Genome Biology*   (2024) 25:311

Page 18 of 20

Data availability
The amplicon sequencing data have been deposited in the NCBI Gene Expression Omnibus database (BioProject ID: PRJNA1077879) and are fully accessible [59]. No other scripts and software were used other than those mentioned in the "Methods" section. The request for reagents will be fulfilled by H. D. (daihsh@outlook.com).

Declarations

Ethics approval and consent to participate
Not applicable.

Consent for publication
Not applicable.

Competing interests
Tongwen Zhang is currently an employee of Boji Biopharmaceutical. The authors declare no competing interests. Neither their employers nor the funding agency had any influence on the study design, data collection, analysis, or interpretation of results.

References

1. Burt A. Site-specific selfish genes as tools for the control and genetic engineering of natural populations. Proc Biol Sci. 2003;270(1518):921–8.
2. Bier E. Gene drives gaining speed. Nat Rev Genet. 2022;23(1):5–22.
3. Price TAR, Windbichler N, Unckless RL, Sutter A, Runge JN, Ross PA, Pomiankowski A, Nuckolls NL, Montchamp-Moreau C, Mideo N, et al. Resistance to natural and synthetic gene drive systems. J Evol Biol. 2020;33(10):1345–60.
4. Cong L, Ran FA, Cox D, Lin S, Barretto R, Habib N, Hsu PD, Wu X, Jiang W, Marraffini LA, et al. Multiplex genome engineering using CRISPR/Cas systems. Science. 2013;339(6121):819–23.
5. Gasiunas G, Barrangou R, Horvath P, Siksnys V. Cas9-crRNA ribonucleoprotein complex mediates specific DNA cleavage for adaptive immunity in bacteria. Proc Natl Acad Sci U S A. 2012;109(39):E2579-2586.
6. Jinek M, Chylinski K, Fonfara I, Hauer M, Doudna JA, Charpentier E. A programmable dual-RNA-guided DNA endonuclease in adaptive bacterial immunity. Science. 2012;337(6096):816–21.
7. Jinek M, Jiang F, Taylor DW, Sternberg SH, Kaya E, Ma E, Anders C, Hauer M, Zhou K, Lin S, et al. Structures of Cas9 endonucleases reveal RNA-mediated conformational activation. Science. 2014;343(6176):1247997.
8. Sternberg SH, Redding S, Jinek M, Greene EC, Doudna JA. DNA interrogation by the CRISPR RNA-guided endonuclease Cas9. Nature. 2014;507(7490):62–7.
9. Gantz VM, Bier E. Genome editing. The mutagenic chain reaction: a method for converting heterozygous to homozygous mutations. Science. 2015;348(6233):442–444.
10. Gantz VM, Jasinskiene N, Tatarenkova O, Fazekas A, Macias VM, Bier E, James AA. Highly efficient Cas9-mediated gene drive for population modification of the malaria vector mosquito Anopheles stephensi. Proc Natl Acad Sci U S A. 2015;112(49):E6736-6743.
11. DiCarlo JE, Chavez A, Dietz SL, Esvelt KM, Church GM. Safeguarding CRISPR-Cas9 gene drives in yeast. Nat Biotechnol. 2015;33(12):1250–5.
12. Xu H, Han M, Zhou S, Li BZ, Wu Y, Yuan YJ. Chromosome drives via CRISPR-Cas9 in yeast. Nat Commun. 2020;11(1):4344.
13. Hammond A, Galizi R, Kyrou K, Simoni A, Siniscalchi C, Katsanos D, Gribble M, Baker D, Marois E, Russell S, et al. A CRISPR-Cas9 gene drive system targeting female reproduction in the malaria mosquito vector Anopheles gambiae. Nat Biotechnol. 2016;34(1):78–83.
14. Kyrou K, Hammond AM, Galizi R, Kranjc N, Burt A, Beaghton AK, Nolan T, Crisanti A. A CRISPR-Cas9 gene drive targeting doublesex causes complete population suppression in caged Anopheles gambiae mosquitoes. Nat Biotechnol. 2018;36(11):1062–6.
15. Grunwald HA, Gantz VM, Poplawski G, Xu XS, Bier E, Cooper KL. Super-Mendelian inheritance mediated by CRISPR-Cas9 in the female mouse germline. Nature. 2019;566(7742):105–9.
16. Walter M, Verdin E. Viral gene drive in herpesviruses. Nat Commun. 2020;11(1):4884.
17. Drury DW, Dapper AL, Siniard DJ, Zentner GE, Wade MJ. CRISPR/Cas9 gene drives in genetically variable and nonrandomly mating wild populations. Sci Adv. 2017;3(5):e1601910.
18. Hammond AM, Kyrou K, Bruttini M, North A, Galizi R, Karlsson X, Kranjc N, Carpi FM, D'Aurizio R, Crisanti A, et al. The creation and selection of mutations resistant to a gene drive over multiple generations in the malaria mosquito. PLoS Genet. 2017;13(10):e1007039.

19. Noble C, Olejarz J, Esvelt KM, Church GM, Nowak MA. Evolutionary dynamics of CRISPR gene drives. Sci Adv. 2017;3(4): e1601964.
20. Esvelt KM, Smidler AL, Catteruccia F, Church GM. Concerning RNA-guided gene drives for the alteration of wild populations. eLife. 2014;3:e03401.
21. Champer SE, Oh SY, Liu C, Wen Z, Clark AG, Messer PW, Champer J: Computational and experimental performance of CRISPR homing gene drive strategies with multiplexed gRNAs. Sci Adv. 2020;6(10):eaaz0525.
22. Bishop AL, Lopez Del Amo V, Okamoto EM, Bodai Z, Komor AC, Gantz VM. Double-tap gene drive uses iterative genome targeting to help overcome resistance alleles. Nat Commun. 2022;13(1):2595.
23. Walter M, Perrone R, Verdin E. Targeting conserved sequences circumvents the evolution of resistance in a viral gene drive against human cytomegalovirus. J Virol. 2021;95(15): e0080221.
24. Lewis IC, Yan Y, Finnigan GC. Analysis of a Cas12a-based gene-drive system in budding yeast. Access Microbiol. 2021;3(12): 000301.
25. Sanz Juste S, Okamoto EM, Nguyen C, Feng X, Lopez Del Amo V. Next-generation CRISPR gene-drive systems using Cas12a nuclease. Nat Commun. 2023;14(1):6388.
26. Stella S, Alcon P, Montoya G. Structure of the Cpf1 endonuclease R-loop complex after target DNA cleavage. Nature. 2017;546(7659):559–63.
27. Kim D, Kim J, Hur JK, Been KW, Yoon SH, Kim JS. Genome-wide analysis reveals specificities of Cpf1 endonucleases in human cells. Nat Biotechnol. 2016;34(8):863–8.
28. Kim DY, Lee JM, Moon SB, Chin HJ, Park S, Lim Y, Kim D, Koo T, Ko JH, Kim YS. Efficient CRISPR editing with a hypercompact Cas12f1 and engineered guide RNAs delivered by adeno-associated virus. Nat Biotechnol. 2022;40(1):94–102.
29. Xu X, Chemparathy A, Zeng L, Kempton HR, Shang S, Nakamura M, Qi LS. Engineered miniature CRISPR-Cas system for mammalian genome regulation and editing. Mol Cell. 2021;81(20):4333-4345.e4334.
30. Wu Z, Zhang Y, Yu H, Pan D, Wang Y, Li F, Liu C, Nan H, Chen W, Ji Q. Programmed genome editing by a miniature CRISPR-Cas12f nuclease. Nat Chem Biol. 2021;17(11):1132–8.
31. Takeda SN, Nakagawa R, Okazaki S, Hirano H, Kobayashi K, Kusakizako T, Nishizawa T, Yamashita K, Nishimasu H, Nureki O. Structure of the miniature type V-F CRISPR-Cas effector enzyme. Mol Cell. 2021;81(3):558-570.e553.
32. Xin C, Yin J, Yuan S, Ou L, Liu M, Zhang W, Hu J. Comprehensive assessment of miniature CRISPR-Cas12f nucleases for gene disruption. Nat Commun. 2022;13(1):5623.
33. Fuchs S, Garrood WT, Beber A, Hammond A, Galizi R, Gribble M, Morselli G, Hui TJ, Willis K, Kranjc N, et al. Resistance to a CRISPR-based gene drive at an evolutionarily conserved site is revealed by mimicking genotype fixation. PLoS Genet. 2021;17(10): e1009740.
34. Champer J, Reeves R, Oh SY, Liu C, Liu J, Clark AG, Messer PW. Novel CRISPR/Cas9 gene drive constructs reveal insights into mechanisms of resistance allele formation and drive efficiency in genetically diverse populations. PLoS Genet. 2017;13(7): e1006796.
35. Hammond A, Karlsson X, Morianou I, Kyrou K, Beaghton A, Gribble M, Kranjc N, Galizi R, Burt A, Crisanti A, et al. Regulating the expression of gene drives is key to increasing their invasive potential and the mitigation of resistance. PLoS Genet. 2021;17(1): e1009321.
36. Carrami EM, Eckermann KN, Ahmed HMM, Sanchez CH, Dippel S, Marshall JM, Wimmer EA. Consequences of resistance evolution in a Cas9-based sex conversion-suppression gene drive for insect pest management. Proc Natl Acad Sci U S A. 2018;115(24):6189–94.
37. Dai HS, Griffin N, Bolyard C, Mao HC, Zhang J, Cripe TP, Suenaga T, Arase H, Nakano I. Chiocca EA *et al*: The Fc domain of immunoglobulin is sufficient to bridge NK cells with virally infected cells. Immunity. 2017;47(1):159-170.e110.
38. Chen SH, Lin YW, Griffiths A, Huang WY. Competition and complementation between thymidine kinase-negative and wild-type herpes simplex virus during co-infection of mouse trigeminal ganglia. J Gen Virol. 2006;87(Pt 12):3495–502.
39. Suenaga T, Kohyama M, Hirayasu K, Arase H. Engineering large viral DNA genomes using the CRISPR-Cas9 system. Microbiol Immunol. 2014;58(9):513–22.
40. Bi Y, Sun L, Gao D, Ding C, Li Z, Li Y, Cun W, Li Q. High-efficiency targeted editing of large viral genomes by RNA-guided nucleases. PLoS Pathog. 2014;10(5):e1004090.
41. Morimoto T, Arii J, Akashi H, Kawaguchi Y. Identification of multiple sites suitable for insertion of foreign genes in herpes simplex virus genomes. Microbiol Immunol. 2009;53(3):155–61.
42. Wisner T, Brunetti C, Dingwell K, Johnson DC. The extracellular domain of herpes simplex virus gE is sufficient for accumulation at cell junctions but not for cell-to-cell spread. J Virol. 2000;74(5):2278–87.
43. Post LE, Roizman B. A generalized technique for deletion of specific genes in large genomes: alpha gene 22 of herpes simplex virus 1 is not essential for growth. Cell. 1981;25(1):227–32.
44. de Felipe P, Martin V, Cortes ML, Ryan M, Izquierdo M. Use of the 2A sequence from foot-and-mouth disease virus in the generation of retroviral vectors for gene therapy. Gene Ther. 1999;6(2):198–208.
45. Kuny CV, Bowen CD, Renner DW, Johnston CM, Szpara ML: In vitro evolution of herpes simplex virus 1 (HSV-1) reveals selection for syncytia and other minor variants in cell culture. Virus Evol. 2020;6(1):veaa013.
46. Schirmer M, Ijaz UZ, D'Amore R, Hall N, Sloan WT, Quince C. Insight into biases and sequencing errors for amplicon sequencing with the Illumina MiSeq platform. Nucleic Acids Res. 2015;43(6):e37.
47. Walter M, Haick AK, Riley R, Massa PA, Strongin DE, Klouser LM, Loprieno MA, Stensland L, Santo TK, Roychoudhury P, et al. Viral gene drive spread during herpes simplex virus 1 infection in mice. Nat Commun. 2024;15(1):8161.
48. Zhao Z, Shang P, Sage F, Geijsen N. Ligation-assisted homologous recombination enables precise genome editing by deploying both MMEJ and HDR. Nucleic Acids Res. 2022;50(11):e62.
49. Morisaka H, Yoshimi K, Okuzaki Y, Gee P, Kunihiro Y, Sonpho E, Xu H, Sasakawa N, Naito Y, Nakada S, et al. CRISPR-Cas3 induces broad and unidirectional genome editing in human cells. Nat Commun. 2019;10(1):5302.
50. Terradas G, Bennett JB, Li Z, Marshall JM, Bier E. Genetic conversion of a split-drive into a full-drive element. Nat Commun. 2023;14(1):191.

51. Stow EC, Stow ND. Complementation of a herpes simplex virus type 1 Vmw110 deletion mutant by human cytomegalovirus. J Gen Virol. 1989;70(Pt 3):695–704.

52. Vastag L, Koyuncu E, Grady SL, Shenk TE, Rabinowitz JD. Divergent effects of human cytomegalovirus and herpes simplex virus-1 on cellular metabolism. PLoS Pathog. 2011;7(7): e1002124.

53. Grosse S, Huot N, Mahiet C, Arnould S, Barradeau S, Clerre DL, Chion-Sotinel I, Jacqmarcq C, Chapellier B, Ergani A, et al. Meganuclease-mediated inhibition of HSV1 infection in cultured cells. Mol Ther. 2011;19(4):694–702.

54. Yin D, Ling S, Wang D, Dai Y, Jiang H, Zhou X, Paludan SR, Hong J, Cai Y. Targeting herpes simplex virus with CRISPR-Cas9 cures herpetic stromal keratitis in mice. Nat Biotechnol. 2021;39(5):567–77.

55. Aubert M, Haick AK, Strongin DE, Klouser LM, Loprieno MA, Stensland L, Santo TK, Huang ML, Hyrien O, Stone D, et al. Gene editing for latent herpes simplex virus infection reduces viral load and shedding in vivo. Nat Commun. 2024;15(1):4018.

56. Zhang T, Jou TH, Hsin J, Wang Z, Huang K, Ye J, Yin H, Xing Y: Talimogene laherparepvec (T-VEC): a review of the recent advances in cancer therapy. J Clin Med. 2023;12(3):1098.

57. Gurevich I, Agarwal P, Zhang P, Dolorito JA, Oliver S, Liu H, Reitze N, Sarma N, Bagci IS, Sridhar K, et al. In vivo topical gene therapy for recessive dystrophic epidermolysis bullosa: a phase 1 and 2 trial. Nat Med. 2022;28(4):780–8.

58. West SA, Griffin AS, Gardner A. Social semantics: altruism, cooperation, mutualism, strong reciprocity and group selection. J Evol Biol. 2007;20(2):415–32.

59. Zhuangjie Lin QY, Keyuan Lai, Kehua Jiao, Xianying Zeng, Guanxiong Lei, Tongwen Zhang, Hongsheng Dai: HSV1 gene drive viruses. Gene Expression Omnibus. PRJNA1077879. 2024. https://www.ncbi.nlm.nih.gov/bioproject/?term=PRJNA1077879.

Publisher's Note